Deep-Sea Research I 56 (2009) 2129–2143

Contents lists available at ScienceDirect

Deep-Sea Research I

journal homepage: www.elsevier.com/locate/dsri

Anomalous hydrographic and biological conditions in the northern South China Sea during the 1997–1998 El Niño and comparisons with the equatorial Pacific

Chun-Mao Tseng [a,*], K.-K. Liu [b], L.-W. Wang [b], G.-C. Gong [c]

[a] Institute of Oceanography, National Taiwan University, P.O. Box 23-13, Taipei 106, Taiwan, ROC
[b] Institute of Hydrological and Oceanic Sciences, National Central University, Jungli 320, Taiwan, ROC
[c] Institute of Marine Environmental Chemistry and Ecology, National Taiwan Ocean University, Keelung 224, Taiwan, ROC

ARTICLE INFO

Article history:
Received 16 July 2008
Received in revised form
3 September 2009
Accepted 13 September 2009
Available online 22 September 2009

Keywords:
Chlorophyll-*a*
Primary production
El Niño
Monsoon
South East Asian Time-series Study (SEATS)
South China Sea

ABSTRACT

It is demonstrated that weakened wind mixing and strengthened water column stratification resulted in the anomalously low sea surface chlorophyll in the northern South China Sea during the 1997–1998 El Niño event. Remotely sensed sea surface temperature, wind and chlorophyll, which were validated by shipboard observations at the SouthEast Asian Time-series Study (SEATS) station (18°N, 116°E) in the northern South China Sea (SCS) provided the basis for this study. During the 1997–1998 winter at the SEATS station, the sea surface temperature was elevated by about 2 °C above the climatological mean, while the wind speed of the northeast monsoon was reduced from a climatological mean of 9.4 to 6.8 m/s. The concentration of surface chlorophyll-*a* dropped from 0.2 to 0.1 mg/m^3. The monthly area-averaged integrated primary production estimated for the northern SCS area (112–119°E, 15–21°N) was reduced by about 40% of the normal winter value. Under the anomalously high sea surface temperature and weak monsoon, the mixed-layer depth would have been reduced from an average of 65 to 45 m and the nutrients in the mixed layer would have been reduced by half, according to observations at the SEATS station in more recent years. During the 1997–1998 El Niño event, the onset of warming in the northern SCS lagged behind that in the eastern equatorial Pacific by about 5 months and lingered for 11 months. This course of change resembled that of the western Pacific warm pool region. However, contrary to the northern SCS, the sea surface chlorophyll was enhanced in the warm pool region during the event, probably mainly because of the uplifted nutricline. Unlike the eastern equatorial Pacific, the dramatic recovery of biological production did not happen in the SCS in the summer of 1998. These distinctive biogeochemical responses reflect fundamental differences between the SCS and the equatorial Pacific in terms of upper water column dynamics.

1. Introduction

The El Niño episodes with a 2–7 year cycle, typically lasting about 12–18 months in each episode (Glantz, 1996), have caused drastic global climate variability and exerted tremendous socio-economic impacts. The El Niño related disturbances and influences on ocean environmental conditions have been gradually unveiled, because

* Corresponding author. Tel.: +886 2 33669775; fax: +886 2 23644049.
E-mail address: cmtseng99@ntu.edu.tw (C.-M. Tseng).

0967-0637/$ - see front matter © 2009 Elsevier Ltd. All rights reserved.
doi:10.1016/j.dsr.2009.09.004

there have been many studies on them over the past decades (e.g., Chavez et al., 2002a, b). During an El Niño episode, sea surface temperature (SST, see Appendix for abbreviations and acronyms used throughout the paper) in the tropical central and eastern Pacific Ocean, is anomalously high (Newell and Weare, 1976). The anomalous warming is accompanied by dramatic changes in marine ecology and fisheries (Joseph and Miller, 1989). It has been reported that the 1997–1998 El Niño event was the strongest one ever recorded (Chavez et al., 2002a, b). During that episode, large-scale weakening of the trade winds and deepening of the nutricline and thermocline occurred, resulting in elevated SST and decreased nutrient and chlorophyll concentrations in surface seawater in the eastern and central equatorial Pacific.

A rich literature has well documented the 1997–1998 El Niño impacts on physics and biogeochemistry of the equatorial Pacific (Chavez et al., 1999; Strutton and Chavez, 2000; Turk et al., 2001; Chavez et al., 2002a, b; Kutsuwada and McPhaden, 2002; Wang et al., 2005b, 2006; Feely et al., 2006). In January 1998, chlorophyll diminished in the eastern equatorial Pacific in the height of the El Niño event. Subsequently, a dramatic recovery of the enhanced chlorophyll occurred in July 1998 (Chavez et al., 1999). The new production over the equatorial Pacific dropped by 30% during the El Niño event and increased by 40% during the subsequent La Niña (Turk et al., 2001). Such dramatic changes were attributed to the anomalously strong depression of the 20 °C isotherm and ferricline during the El Niño and the rapid recovery in the ensuing period (Turk et al., 2001; Wang et al., 2005b).

The Western Pacific Warm Pool (WPWP, SST greater than 28 °C) is a large area of ocean centered in the seas around Indonesia (60–170°E, 15°N–15°S). This region contains the warmest ocean water in the world and slowly fluctuates in size (Yan et al., 1992; Picaut and Delcroix, 1995). Many studies have addressed its importance and impact on the development and strength of the El Niño event and further global climate variability (McPhaden and Picaut, 1990; Picaut et al., 1996; Touree and White, 1997). In contrast to the eastern equatorial Pacific, biological production in the WPWP was enhanced during the 1997–1998 El Niño event (McClain et al., 1999; Murtugudde et al., 1999).

Relatively few publications have reported what happened in the western Pacific marginal seas, even though these marginal seas, including the SCS, are sensitive to climate variations (e.g., Chao et al., 1996) and bear rich records of paleo-climate changes (e.g., Wang et al., 2005a). During the 1997–1998 El Niño, the Taiwan Strait, which connects the East China Sea (ECS) to the north and the South China Sea (SCS) to the south, suffered from anomalous warming (Kuo and Ho, 2004), which was accompanied by decreased nutrient supply and, consequently, diminished sea surface chlorophyll-*a* (S-chl) (Shang et al., 2005). This was attributed to a reduced southward transport of the cold, fresh and nutrient-rich Zhe-Min Coastal Water (ZMCW) from the ECS under a weaker northeast monsoon in the winter. By contrast, the intrusion of the warm, saline and nutrient-poor South China Sea Warm Water (SCSWC) from the SCS was enhanced, leading to anomalous warming and reduced phytoplankton growth. Therefore, the occurrence of an El Niño could affect not only the hydrography but also the ecology in the Taiwan Strait. Based on satellite remote sensing, Zhao and Tang (2007) reported anomalously high SST and low chlorophyll offshore along the Vietnamese coast between 10° and 16°N in the summer of 1998 and attributed the anomaly to the 1997–1998 El Niño event. Tseng et al. (2009) reported similar observations at the SouthEast Asian Time-series Study (SEATS) station in the northern SCS during the two El Niño events between 1997 and 2003 with little discussion of the mechanism. Since the 1997–1998 El Niño event exerted considerable impacts upon the SCS and adjacent Taiwan Strait, we deem it worthwhile to provide an in-depth discussion of the processes that lead to changes in phytoplankton biomass and primary productivity in the northern SCS and to compare these conditions with those observed in the equatorial Pacific Ocean. The circulation in the SCS is briefly described below to facilitate the discussion.

The circulation in the SCS is subject to forcing of alternating monsoons (Fig. 1). The northeast monsoon in winter drives a cyclonic gyre around the basin; the southwest monsoon in summer causes reversal of the gyre in the southern part of the basin, but the northward flowing coastal jet off Vietnam tends to veer off the coastal zone (Shaw and Chao, 1994). The Kuroshio intrusion occurring in winter (Shaw, 1991; Centurioni et al., 2004) brings nutrient-poor water to the upper water column of the SCS from the West Philippine Sea (WPS) (Gong et al., 1992). Besides the surface intrusion, there is a deep inflow into the SCS from the WPS at sill depth around 2000 m through the Luzon Strait, with an estimated transport of about 1 Sv (Wang, 1986; Liu and Liu, 1988; Gong et al., 1992). The North Pacific Intermediate water (You et al., 2005; Qu et al., 2006) also enters the SCS. The deep and intermediate water inflows induce a basin-wide upwelling. In the upper water column, the monsoons drive upwelling in three regions: off northwestern Luzon and around the shelf break in northern Sunda Shelf in winter and off the central Vietnamese coast in summer (Chao et al., 1996; Shaw et al., 1996). The nitrate fluxes associated with upwelling have been estimated by Liu et al. (2002) using a coupled physical–biogeochemical model. Each of the three upwelling regions has an area of about 2×10^5 km^2, which gives a total upwelled nitrate on the order of 1 Gmol/day in each region during the corresponding upwelling season. The upwelling of the subsurface water is a major source of nutrients for supporting primary production in the SCS (Liu et al., 2002, 2009). Aside from exchanges through the Luzon Strait, the upper water column of the SCS also exchanges water through other straits and channels, such as the Mindoro Strait (Liu et al., 2009). Most notable are exchanges of the surface water with the shallow Java Sea over the Sunda Shelf (Fig. 1).

Here, we report the hydrographic and biological conditions in the northern SCS by using remote sensing data from 1997 to 2003 and field observations at the SEATS station. This period contains the 1997–1998 El Niño episode. The dataset allows us to examine the impact of

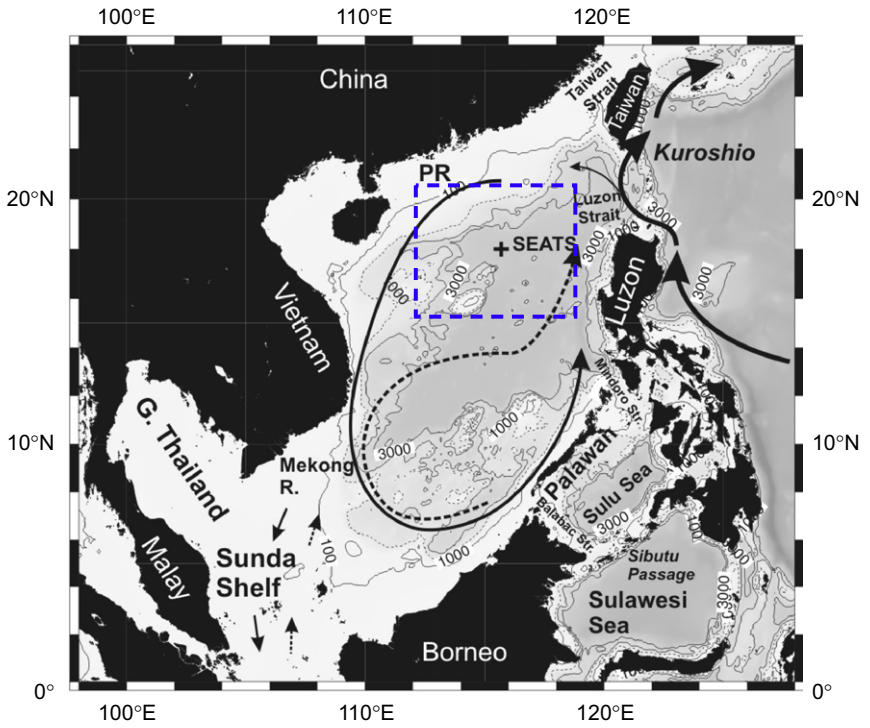

Fig. 1. Topography of the South China Sea (SCS) and surrounding seas with major surface currents marked (modified after Liu et al., 2009). Also shown are the location of the Southeast Asian Time-series Study (SEATS) station and the study region (Dashed square: Box S, 112–119°E and 15–21°N) in the northern South China Sea. Within the SCS: Solid curves—currents in the winter; Dashed curves—currents in the summer. The flow path of the Kuroshio and its intrusion into the South China Sea are also shown.

the El Niño event upon hydrographic and biogeochemical conditions in the northern SCS, which may be compared with conditions in the equatorial Pacific Ocean. The purpose is to better understand the response of the biogeochemical system of the northern SCS to changes in physical forcing. Such understanding will shed light on biogeochemical feedback of tropical–subtropical marginal seas during climate change.

2. Materials and methods

2.1. Field observations

The SEATS station, located at 18°N and 116°E (Fig. 1), was occupied 19 times in approximately seasonal intervals between September 1999 and October 2003. During each occupation of the station, the distributions of salinity, temperature and photosynthetically available radiation (PAR) were recorded with a SeaBird conductivity–temperature–depth (CTD) recorder and a Biospherical quantum scalar irradiance sensor. The mixed-layer depth (MLD) and the euphotic zone depth (EZD) during each cruise were estimated as the depth above which the density gradient was $\leq 0.1\ \sigma_\theta$ (unit m^{-1}) and the depth at which the PAR had been reduced to 1% of the surface value, respectively (Tseng et al., 2005).

Discrete seawater samples were collected with depth in GO-FLO bottles that were mounted onto a Rosette sampling assembly (General Oceanic). Subsamples were quick-frozen with liquid nitrogen on board ship and returned to a shore-based laboratory for the determination of (nitrate+nitrite), (N+N) and soluble reactive phosphate, SRP. Nitrate+nitrite was determined by the standard pink azo dye method that had been adapted for use with a flow injection analyzer (Strickland and Parsons, 1984; Pai et al., 1990). Soluble reactive phosphate was determined manually with the standard molybdenum blue method (Strickland and Parsons, 1984). The precision and detection limit for the determination of (N+N) and SRP by using a 10-cm flowing cell were both similarly $\pm 1\%$ and 0.01 μM, respectively. The depth at the top of the nutricline (TND) was defined as the *x*-intercept of a plot of (N+N) in the nutricline against depth (Tseng et al., 2005). Separate subsamples were filtered onboard ship. The filters were stored at −20 °C and then returned to the shore-based laboratory for the fluorometric determination of chlorophyll-*a* (Chl-*a*) (Strickland and Parsons, 1984). Primary production was determined by measuring the uptake of added $H^{14}CO_3^{-1}$ during the incubation of discrete water samples at six depths within the top 100 m of the water column under trace-metal-clean condition. The euphotic zone depth-integrated inventories of chlorophyll-*a* (I-chl) and primary production (IPP) were estimated by the trapezoidal method.

The archived shipboard SST in the vicinity of the SEATS station between 1992 and 2004 were obtained from the Ocean Data Bank of the National Center for Ocean

Research of Taiwan. They provided data from a total number of 26 stations located at or near the SEATS station within the area of 115–116°E and 18–19°N. The length of the field-observed SST record covered the period of the 1997–1998 El Niño event. The data quality of the remote sensing SST data set was further calibrated by the field-observed CTD data.

2.2. Remote sensing data at the SEATS station location and in the equatorial Pacific

The daily averaged sea surface temperature (SST), air temperature (AT) at 2 m above the sea surface and wind vector at or near the location of the SEATS station (115–116°E, 18–19°N) and in the northern SCS region (Box S, 15–21°N and 112–119°E) between January 1986 and December 2003 were obtained from the National Oceanic and Atmospheric Administration (NOAA) through NCEP (National Center for Environmental Prediction). Surface chlorophyll-*a* (S-chl) and PAR data between September 1997 and December 2003 were retrieved from SeaWiFS (Sea-viewing Wide Field-of-view Sensor) level 3 Standard Mapped Image (SMI) of chlorophyll-*a* concentration and PAR data, respectively, with a spatial resolution of 9 km. They all were well-validated higher-level products obtained from Goddard Earth Sciences-Distributed Active Archive Center (GES-DAAC), SeaWiFs Project, National Aeronautics and Space Administration (NASA) (http://oceancolor.gsfc.nasa.gov/ftp.html). The records of SeaWiFS data began just in time to cover the El Niño event in 1997–1998. The modeled IPP data were estimated from the SeaWiFS-derived S-chl and PAR data by the empirical vertical production model developed for the East Asia marginal seas (Gong et al., 2003). The SeaWiFS S-chl data were calibrated against the field-observed data (Tseng et al., 2005). The NCEP-SST, -AT and -wind speed (WS) all agreed well with shipboard observations (Tseng et al., 2005). It indicates the remote sensing data used here are reliable and validated in terms of data assurance.

Please note to have a comparison between the SEATS/SCS and two sites in the Equatorial Pacific Ocean, the remote sensing monthly data such as SST, AT, and WS and SeaWiFS S-chl in the regions of the Niño3 (150–90°W, 5°S–5°N) and WPWP (60–170°E, 15°N–15°S) used in the study period between January 1986 and December 2003 were all obtained from NOAA-NCEP and NASA-GES-DAAC, respectively.

2.3. Index for the occurrence of El Niño

The monthly average SST anomaly between January 1986 and December 2003 in the Niño 3.4 region (170–120°W, 5°S–5°N), provided by the National Oceanic and Atmospheric Administration (NOAA) through NCEP at the web-site "http://www.cpc.ncep.noaa.gov/data/indices/sstoi.indices", was used as an index for identifying the occurrence of El Niño events. An El Niño event occurred when the 5-month running mean of SST anomaly exceeded +0.4 °C for 6 or more consecutive months (Trenberth, 1997).

2.4. Index for the SST variance of the western Pacific warm pool

The Warm Pool (WP) index as 1st EOF of SST in the WPWP region was provided by Climate Diagnostics Center, NOAA-CIRES at the web-site "http://www./cdc.noaa.gov/data/climateindices/list/#WP". The monthly SST data were analyzed for the period 1950–present and were subjected to an empirical orthogonal function (EOF) analysis to derive an objective index of the state of the Western Pacific Warm Pool. As described previously by Hoerling et al. (2001), the time series of the 1st EOF mode of SST was found to correlate highly with other widely used indices of ENSO for the tropical Pacific Ocean (120°E–60°W, 20°N–20°S).

2.5. Environmental anomalies

The inter-annual variability in environmental variables at the sites of the SEATS/SCS, Niño3 and WPWP was depicted by anomalies. In order to accentuate the longer term seasonal and inter-annual variations, the monthly average anomalies were presented. Firstly, the climatological monthly mean SST, WS, S-chl and IPP (MIP) were calculated for each month of the year. Then, the anomalies in SST (SSTA), WS (WSA), S-chl (S-chlA) and MIP (MIPA) were computed as the difference between the observed and climatological means for the particular month in the year.

3. Results

3.1. Seasonal patterns of wind and SST

Time-series data of monthly mean wind speed (WS) and SST at the SEATS station from 1986 to 2003 are plotted in Figs. 2a and b. Also plotted in the same figures are data from shipboard observations of WS and SST, which agree with and validate the NCEP Re-analysis data. Since the air temperature followed SST closely, it is not shown in the figures to avoid filling the figures with too much information. For comparison data from two additional areas in the equatorial Pacific are presented (Fig. 2c–f). One is the WPWP area, 15°S–15°N and 60–170°E. The other is the Niño3 area, 5°S–5°N and 150–90°W, which represents the eastern equatorial Pacific (Wang et al., 2005b). The wind is a main driver of the upper ocean dynamics, while the SST reflects the physical conditions at the study sites. The contrasts in seasonality between the SEATS station and the two Equatorial Pacific sites are summarized in Table 1. Also plotted is the Niño3.4 Index (Fig. 2g), which shows the ENSO events marked as colored stripes.

The wind pattern at the SEATS station was governed by the monsoons: the northeast monsoon in the winter and the southwest monsoon in the summer. Consequently, the wind speed in the SCS usually showed two peaks annually (Table 1, Fig. 2a). The WS during the northeast monsoon, averaging 9.4 m/s, was higher than that, averaging 5.7 m/s, during the southwest monsoon. The lowest WS was found in

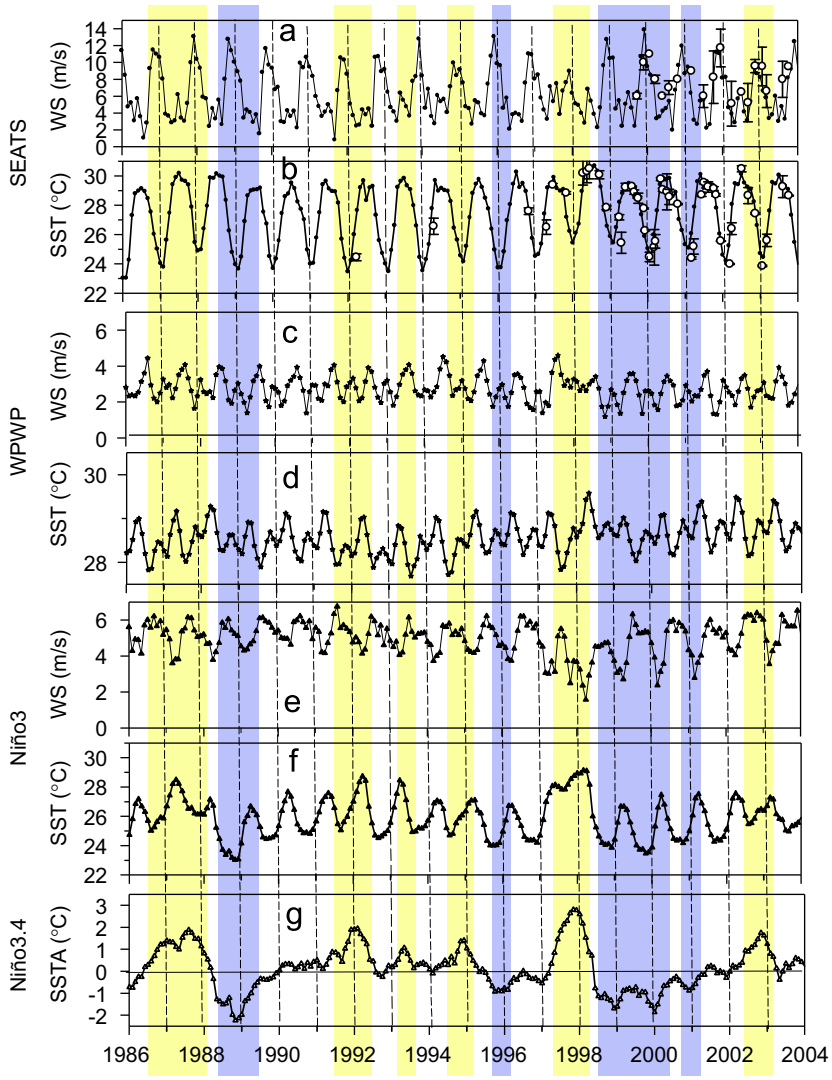

Fig. 2. Variations in (a) wind speed (WS, ●) and field-observed WS (○), and (b) remotely sensed sea surface temperature (SST, ●) and field-observed SST (○) at the SEATS station; (c) WS and (d) SST in the Western Pacific Warm Pool (WPWP); (e) WS and (f) SST in the Niño3 region; (g) SSTA in the Niño3.4 region between 1986 and 2003. The ENSO events are marked as colored stripes: El Niño events in yellow and La Niña in blue.

the inter-monsoonal periods in the late spring (April–May) and the early fall (September–October). The SST oscillated between 23 and 31 °C seasonally with lows at 23–25 °C in winter and highs at 29–31 °C in summer.

The wind pattern in the WPWP area also showed two peaks annually similar to that of the SCS, but the wind speed contrast was the opposite, stronger in the boreal summer and weaker in the boreal winter (Table 1, Fig. 2c). Besides, the wind was much weaker, compared to the SCS, with a mean WS of about 3 m/s and a small seasonal amplitude of about 2 m/s. The SST oscillated seasonally between 27.5 and 29.5 °C with a mean seasonal amplitude of only about 1 °C. It is interesting to note that the SST showed two peaks annually, which matched the wind speed minima in spring and fall (Table 1).

In the Niño3 region, the wind pattern usually showed a single annual peak in boreal summer with a seasonal amplitude of about 2 m/s (Table 1, Fig. 2e). The annual mean was 5 m/s. The SST oscillated between 23 and 29 °C with a mean seasonal amplitude of 2.6 °C. The SST minima, signifying the maximal upwelling in the eastern Equatorial Pacific, occurred in boreal summer corresponding to the wind speed maxima with a slight time lag. By contrast, the SST maxima occurred in boreal spring corresponding to the wind speed minima.

During the 1997–1998 El Niño event the winter peak of wind speed at the SEATS station was the lowest among all winter peaks, while the SST minimum was the highest among all the lows. By contrast, wind in the WPWP region was anomalously strong so that the WS never died down in the boreal fall of 1997 and stayed at about 3 m/s, when the WS usually dropped to 2 m/s or less. The mid-year SST minimum in 1997 was lower than most lows, while the SST in early 1998 reached a maximum above all highs. In the Niño3 region, the wind was anomalously weak and in directions unfavorable for equatorial upwelling (Chavez

Table 1
Comparison of seasonality in environmental variables and 1997–1998 El Niño winter[a] with climatological winter between SEATS station and WPWP and Niño3 regions.

Variables	SEATS (115–116°E; 18–19°N)	WPWP (170–60°E, 15°S–15°N)	Niño3 (150–90°W, 5°S–5° N)
WS			
Seasonality			
Mean[b]	6.3±2.9	2.8±0.6	5.0±0.7
(Median)	(5.2)	(2.6)	(5.2)
1st max[c]	11.3±1.4 (Dec.),	3.9±0.4 (Aug.),	5.9±0.5 (Aug.)
2nd max	5.0±1.3 (June)	2.9±0.3 (Jan.)	
1st min	2.7±0.9 (Sept.),	2.0±0.5 (Nov.),	3.8±0.7 (Apr.)
2nd min	2.9±0.7 (May)	2.1±0.4 (Apr.)	
Peak#	2	2	1
El-Niño winter	6.8±2.0	3.1±0.2	3.5±0.3
	(73%)[d]	(113%)	(73%)
Clim. winter mean	9.4±1.9	2.7±0.2	4.9±0.4
SST			
Seasonality			
Mean	27.4±2.1	28.5±0.3	25.9±1.0
(Median)	(27.9)	(28.5)	(25.6)
1st max	29.5±0.5 (July)	29.1±0.2 (Apr.)	27.5±0.7 (Apr.)
2nd max		28.7±0.2 (Nov.)	
1st min	24.2±0.7 (Jan.)	28.0±0.2 (Aug),	24.9±0.9 (Sept.)
2nd min		28.4±0.2 (Feb.)	
Peak#	1	2	1
El-Niño winter	25.9±0.4	28.7±0.1	28.9±0.1
	(105%)	(101%)	(112%)
Clim. winter mean	24.6±0.6	28.5±0.1	25.7±0.6
S-chl			
Seasonality			
Mean	0.10±0.04	0.15±0.1	0.12±0.01
(Median)	(0.09)	(0.14)	(0.12)
1st max	0.19±0.07 (Jan.)	0.18±0.02 (Aug.),	0.14±0.02 (Sept)
2nd max		0.15±0.01 (Jan.)	0.14±0.02 (Mar.)
1st min	0.05±0.01 (June)	0.14±0.01 (Mar.),	0.11±0.02 (Dec.)
2nd min		0.14±0.01 (Nov.)	0.12±0.01 (May)
Peak#	1	2	2
El-Niño winter	0.08±0.01	0.16±0.01	0.07±0.02
	(50%)	(110%)	(57%)
Clim. winter mean	0.16±0.03	0.14±0.003	0.11±0.01

[a] Winter months: December, January, February.
[b] Mean denotes annual mean.
[c] Max and min stand for seasonal maximum and minimum of monthly values.
[d] The percent in parenthesis denotes the percent of the climatology winter mean.

et al., 1999). The SST remained anomalously high throughout the event. After mid 1998, the wind was still weaker than usual, even weaker than that in 1997, but its direction turned to favor upwelling (Chavez et al., 1999) and the SST dropped precipitously.

3.2. Seasonal variation of upper water column conditions

The records of observed MLD, EZD and TND, the mixed-layer SRP and N+N, I-chl, IPP and S-chl at the SEATS station are plotted in Fig. 3. Also shown are S-chl data from SeaWiFS for the SEATS site (Fig. 3d) as well as those for the two Equatorial Pacific regions (Figs. 3e and f). All parameters, except EZD and TND, for the SEATS site follow distinctive seasonal patterns as illustrated previously in shorter records (Tseng et al., 2005).

The observed MLD fluctuated between a low of 15–40 m in most of the year and a high of up to 95 m in the winter. By contrast, both TND and EZD stayed within narrow ranges of 42–70 m (average=55±8 m) and 75–95 m (average=85±6 m), respectively. The averages of observed MLD in the summer and the winter were 25±9 and 71±17 m, respectively. The EZD was always deep enough so that the availability of light was unlikely to be the limiting factor of phytoplankton growth in the upper water column. On the other hand, the fluctuations in MLD were so strong that it was sometimes larger than TND and less in other times. When MLD exceeded TND occurring in winter, nutrient would be mixed into the surface layer to enhance phytoplankton growth. Under the reverse situation that prevailed in summer, the subsurface nutrient reserve could not mix into the surface layer efficiently, causing nutrient availability to become the limiting factor of photosynthetic activities.

This explains the observed winter maxima of the mixed-layer N+N (0.2–0.4 μM) and SRP (0.02–0.04 μM) and summer minima around their respective detection limits as shown in Fig. 3b. As the mixed-layer nutrients increased in the winter, S-chl ($>0.2\,mg/m^3$), I-chl

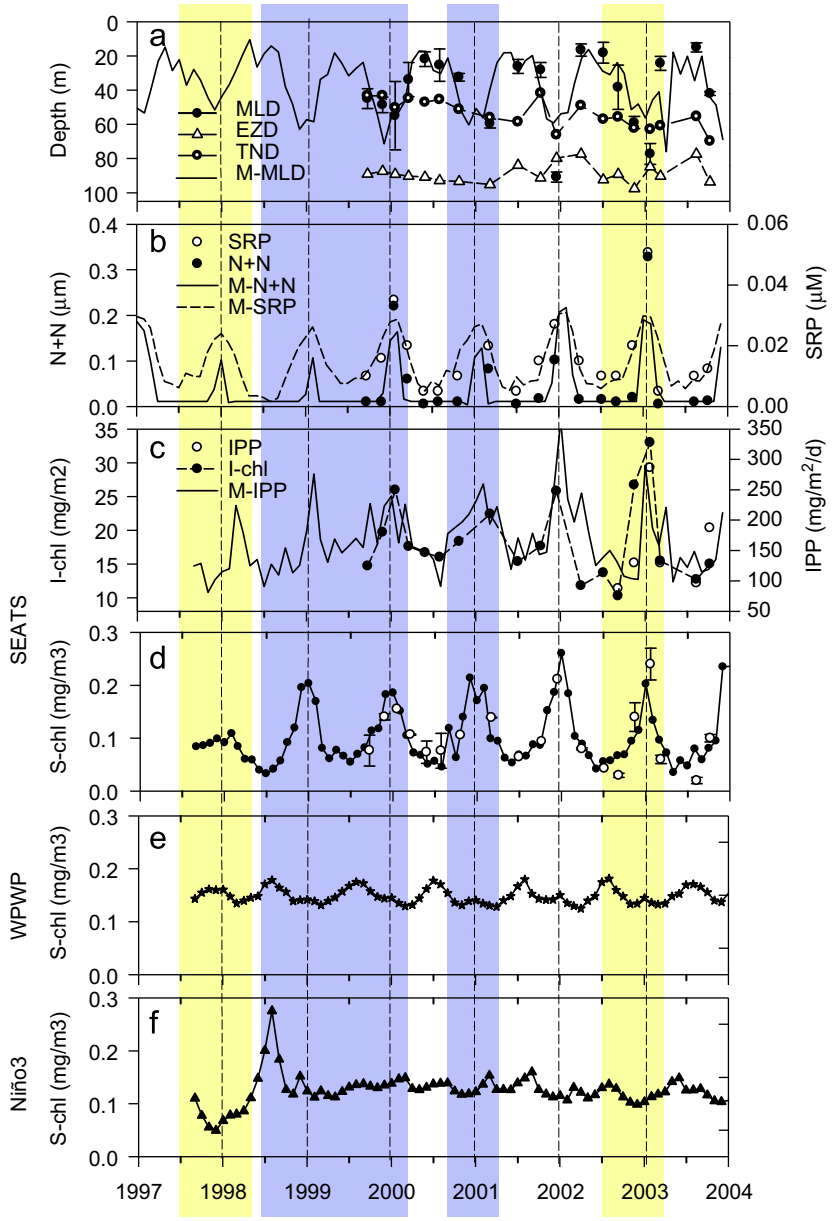

Fig. 3. Variations in (a) mixed-layer depth (MLD, ●), euphotic zone depth (EZD, △), top of nutricline depth (TND, ○), and MLD computed from SST and WS (M-MLD, —), (b) averaged mixed-layer SRP (○) and (N+N) (●), and N+N (M-N+N, —) and SRP (M-SRP, ——) computed from SST, (c) IPP (○), I-chl (●) and IPP (M-IPP, —) derived from S-chl, and (d) SeaWiFs-derived (●) and field-observed (○) S-chl at the SEATS station, (e) SeaWiFs-derived S-chl in the WPWP and (f) Niño3 regions between 1997 and 2003. The ENSO events are marked as in Fig. 2.

($>25\,mg/m^2$) and IPP ($>250\,mg\text{-}C/m^2/d$) reached a maximum, whereas, in the summer, they dropped to a low of S-chl ($<0.1\,mg/m^3$), I-chl ($<15\,mg/m^2$) and IPP ($<150\,mg\text{-}C/m^2/d$). The S-chl from SeaWiFS agreed well with shipboard observations and extended the data coverage to as early as September 1997.

Compared to the strong seasonal variation, the S-chl data for the two equatorial regions exhibit much weaker seasonality (Figs. 3e and f). In fact, the S-chl data in the Niño3 region showed a hardly discernible seasonal pattern (Fig. 3f). On the other hand, they exhibited very strong inter-annual variation, especially during the 1997–1998 ENSO events.

3.3. Anomalies during El Niño events

The records of monthly WS anomaly at the SEATS station and two equatorial Pacific regions are plotted in Fig. 4a. The corresponding records of monthly SST anomaly are plotted in Fig. 4b. The Niño 3.4 index ($SSTA_{N3.4}$) and WP index are plotted in Fig. 4c. The El

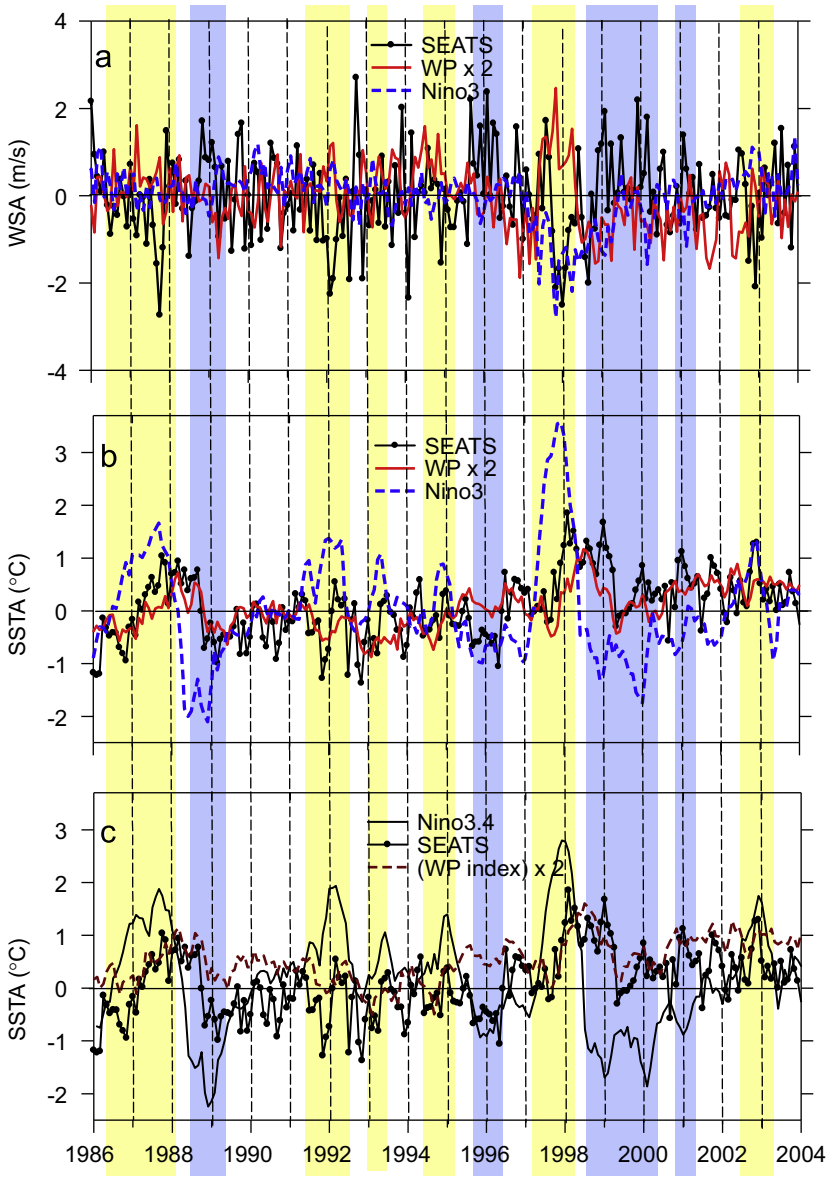

Fig. 4. Anomalies in (a) WS (WSA) at the SEATS site (-●-), in the WP (× 2, —) and Niño3 (—), (b) SST (SSTA) at the SEATS (-●-), in the WP (× 2, —) and Niño3 (—), and (c) SST (SSTA) at the SEATS (-●-), the Niño 3.4 (—) and WP index (× 2, – – –) between 1986 and 2003. The ENSO events were marked as in Fig. 2. The WP (WP index) × 2 denotes two times SSTA values of the WP (WP index).

Niño events in 1986–1988, 1991–1995, 1997–1998 and 2002–2003 are marked according to the Niño3.4 index. So are the La Niña events in 1988–1989, 1995–1996, and 1998–2001. The maximum SST anomalies in the Niño3 region preceded the Niño3.4 index by about 1 month, whereas the WP index followed the Niño3.4 index with a 2–5-month time lag (Fig. 4c). The WP index as 1st EOF of SST can represent the SST anomalies of the WPWP region, as the changes of the WP index were closely in phase with those in SSTA in the WPWP (Figs. 4b and c). An excellent relationship exists between the values of WP index and $SSTA_{WP}$ in the WPWP region from 1986 to 2003 as shown in the following:

$$SSTA_{WP} = 0.95(\pm 0.01) \times WP_{index} - 0.22(\pm 0.01),$$
$$r^2 = 0.94, \quad n = 276 \qquad (1)$$

The 1997–1998 El Niño event was one of the strongest on record as the maximum $SSTA_N$ reached almost $+3\,^{\circ}C$. Correspondingly, in the vicinity of the SEATS location, periods of negative WSA and positive SSTA were recorded in 1986–1988, 1992–1993, 1997–1998 and 2002–2003. These periods corresponded approximately to the El Niño events as indicated by $SSTA_{N3.4}$. Furthermore, the maximum WSA, about -3 m/s, and maximum SSTA of about $+2\,^{\circ}C$

were found during the 1997–1998 event. These similarities are consistent with a linkage between the occurrence of El Niño events and changes in the meteorological and hydrographic conditions in the vicinity of the SEATS station so that WS was reduced and SST was elevated during an El Niño event as indicated in previous reports (Chao et al., 1996; Wang et al., 2002). The $SSTA_{N3.4}$ record also indicated the occurrences of La Niña events when the $SSTA_{N3.4}$ became negative. However, less significant corresponding changes in WSA and SSTA were found in these years. The SSTA in the vicinity of SEATS station during El Niño events were closely related to the WP index (r=0.59, $p<0.0001$; Table 2) and, therefore, showed several months' delay following the Niño3.4 index.

To illustrate the relationship between changes in the vicinity of SEATS station and those in the equatorial Pacific regions during the 1997–1998 event more clearly, we plot the anomalies from all study sites in an expanded time scale from 1997 to mid 2001 (Fig. 5). In the 1997–1998 event, a positive $SSTA_{N3.4}$ became detectable in April 1997 (Fig. 5b). It reached a maximum in December 1997 before dropping back to zero in May 1998. The onset of positive SSTA at the SEATS location and the WP index lagged behind that of $SSTA_{N3.4}$ by about 5 months and did not become evident until September 1997 (Fig. 5b). The positive SSTA and WP index also lingered on for a longer period of time and did not return to zero until April 1999, about 11 months after $SSTA_{N3.4}$. The fact that SSTA was slightly out of phase with $SSTA_{N3.4}$ was not unreasonable since $SSTA_{N3.4}$ reflected changes in the hydrographic condition in the eastern Pacific, an ocean away from the SEATS location. It is worth noting that, during the 1997–1998 El Niño event, SSTA at the SEATS station changed in a way similar to the WP index (Fig. 4c) and also to the SSTA of the WPWP region (Fig. 5b). There were annual maxima and minima in SSTA as observed at the SEATS station, while there were not obvious annual peaks in the SSTA of the WP region (Fig. 5b). The maxima were found during the monsoonal seasons, and the minima corresponded to the intermonsoonal periods. Compared to the variations of SSTA, the WSA variations were more noisy (Figs. 4a and 5a). Again, a very strong and lasting negative WSA was present during the 1997–1998 winter, when the northeast monsoon dropped by about a quarter in strength from a climatological mean of about 9.4 to 6.8 m/s.

The records of S-chl anomaly are compared in Fig. 5c. The most striking feature in the record for the SEATS station was the large and sharp spike of negative S-chlA during the winter in this El Niño event, when S-chl was reduced from the climatological mean by about a half from about 0.2 to 0.1 mg/m^3 (Fig. 3d), yielding a S-chlA of -0.1 mg/m^3 (Fig. 5c). The drop was even deeper than that recorded in the Niño3 region. The onset of the negative S-chlA at the SEATS station occurred in November 1997 (Fig. 5c), but that in the eastern equatorial Pacific was difficult to determine. This is because the SeaWiFS data did not start until September 1997, when the S-chlA in the Nino3 region was already in the negative phase (Fig. 5c). However, it probably occurred sometime between June and September 1997 according to mooring data (Chavez et al., 1999). Therefore, the onset of negative S-chlA at the SEAS station lagged behind that of the Nino3 region by 2–5 months, similar to the course of variation of the SSTA. The negative S-chlA was contrary to the record from the WPWP region, where the S-chl anomaly was positive during the event. It is interesting to note that the onset of the positive S-chlA in the WP region matched the onset of the negative S-chlA at the SEATS station. In the summer of 1998, the negative S-chlA persisted in the northern SCS, though it was more modest. However, the condition was quite different in the WPWP region, where there was essentially no S-chl anomaly. It was also very different in the Niño3 region, where there was a strong positive S-chl anomaly. These contrasts deserve careful discussion.

4. Discussion

4.1. Representativeness of SEATS site for the northern SCS

Through time-series records, we observed that the occurrence of an El Niño in the winter of 1997–1998 could

Table 2
Regression results of monthly average anomalies in environmental variables at the SEATS, NSCS and WPWP with each other from 1986 to 2003.

Variable anomaly	Location	SEATS (115–116°E, 18–19°N)	NSCS (112–119°E, 15–21°N)	WPWP (60–170°E, 15°N–15°S)[a]	WP index (60–170°E, 15°N–15°S)[a]
SSTA[b]	SEATS	1			
	NSCS	0.96	1		
	WPWP	0.59	0.60	1	
	WP index	0.59	0.60	0.97	1
ATA	SEATS	1			
	NSCS	0.98	1		
	WP	0.53	0.52	1	
	WP index	0.56	0.57	0.86	1
WSA	SEATS	1			
	NSCS	0.97	1		
	WPWP	−0.20	−0.17	1	
	WP index	–	–	–	–

[a] WP index denotes 1st EOF of the western Pacific warm pool's SST.
[b] Monthly average anomalies in SST (SSTA), AT (ATA) and WS (WSA) were computed according to the method section of "environmental anomalies".

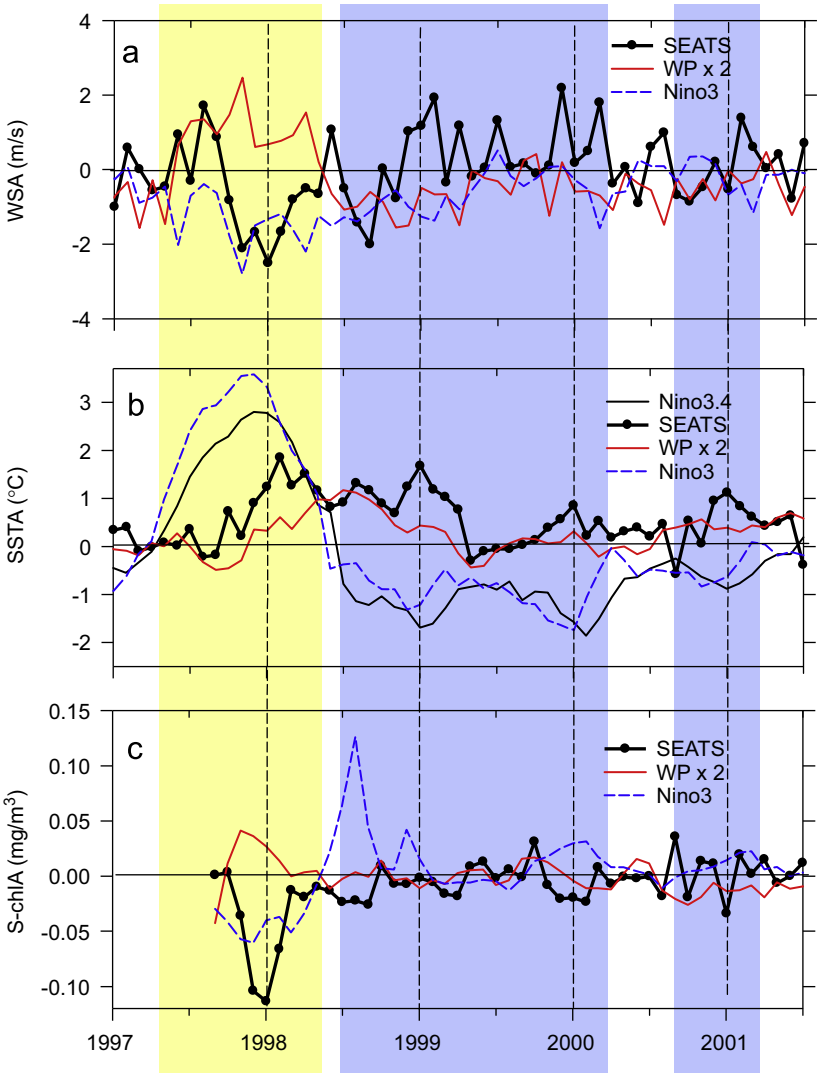

Fig. 5. Anomalies in (a) WS (WSA) at the SEATS (-●-), in the WP (× 2, —) and Niño3 (—), (b) SST (SSTA) at the SEATS (-●-), in the WP (× 2, —), Niño3 (—), and Nino3.4 (—) (c) S-chl (S-chlA) at the SEATS (-●-), the WP (2, —) and Niño3 (—) between 1997 and 2001. The ENSO events were marked as in Fig. 2. The WP × 2 denotes two times SSTA values of the WP.

affect the hydrography and biological conditions at the SEATS station. The significance of the SEATS station for better understanding of inter-annual variation in the biogeochemistry of the whole SCS was apparently manifested (Wong et al., 2007a, b; Tseng et al., 2007). It is conceivable that the effect of the El Niño could have occurred not only at the SEATS station but also in the whole northern SCS. Comparisons of remotely sensed SST and S-chl on monthly average between the SEATS station and in the study area of northern SCS (Box S, 112–119°E and 15–21°N) from September 1997 to December 2003 were carried out. The representativeness of the SEATS station with respect to the hydrography and biological conditions was validated by the regression analysis of monthly averaged SST and S-chl. The results show excellent relationships between values of remotely sensed SST from the SEATS station and northern SCS and between values of S-chl as shown in the following:

$$(\mathrm{SST})_{\mathrm{NSCS}} = 0.99(\pm 0.02) \times (\mathrm{SST})_{\mathrm{SEATS}},$$
$$r^2 = 0.96,\ N = 76,\ p < 0.0001 \quad (2)$$

$$(\mathrm{S-chl})_{\mathrm{NSCS}} = 0.94(\pm 0.02) \times (\mathrm{S-chl})_{\mathrm{SEATS}},$$
$$r^2 = 0.86,\ n = 76,\ p < 0.0001 \quad (3)$$

They indicate that the hydrographic and biological response to the El Niño effect at the SEATS station were closely in phase with those in the northern SCS (Table 2). Therefore, the processes controlling the biogeochemistry of the northern SCS are probably consistent with those governing that in the vicinity of the SEATS station.

Fig. 6 shows the comparison of the modeled IPP results, estimated from the SeaWiFS-derived S-chl and PAR data, during the normal winter (December 2001) and El Niño

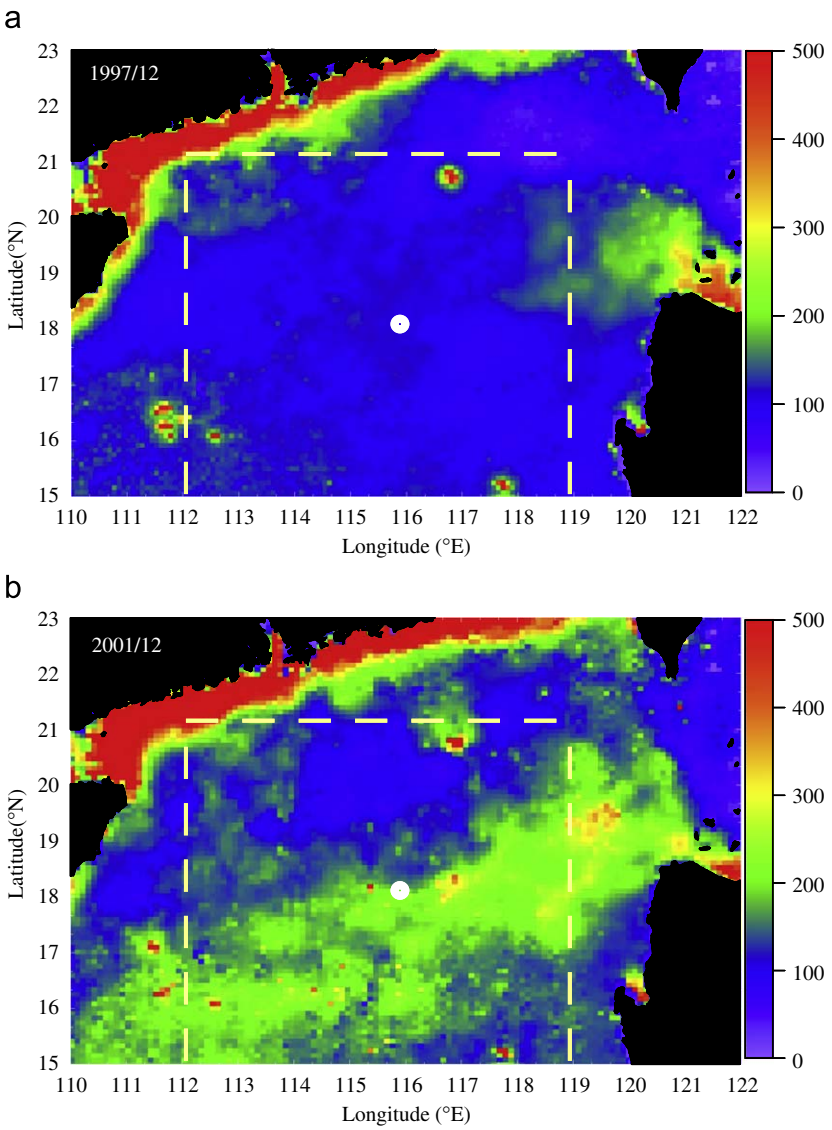

Fig. 6. Comparison of model-derived IPP results in the northern SCS between (a) the El-Niño (December 1997) and (b) normal winter (December 2001). Open circle: SEATS station; Dashed square: Box S

winter (December 1997). Briefly, the monthly average IPP (MIP) near the SEATS station are about 140 and 270 mg-C/m^2/d in the December of 1997 and 2001, respectively. Additionally, the area-averaged MIP in the Box S of the northern SCS dropped by almost 40% of the normal winter condition due to the 1997–1998 El Niño warm event. The anomaly was consistent with the reduction of S-chl and IPP at the SEATS station during the El Niño event (Figs. 3c and d). Again, anomalies observed at the SEATS station are representative for the expanded area in the northern SCS demonstrating that the El Niño event had significant impact on biogeochemical conditions in the northern SCS.

4.2. Potential mechanisms

Tseng et al. (2005) suggested the MLD at the SEATS station in the northern SCS was mainly controlled by surface cooling and wind-induced mixing. The thickening of the MLD in winter was observed due to enhanced vertical mixing by decreasing SST and increasing WS. On the other hand, in general, the concentrations of the nutrients are known to decrease with increasing temperature until it reaches undetectable levels above a certain temperature (Tseng et al., 2005). Thus, during an El Niño event in the northern SCS, as SST increases and WS decreases, MLD should decrease and the concentration of the nutrients should decrease. The assumption on the mixed-layer development has been quantitatively validated by the multiple regression analysis of the observed MLD obtained on the SEATS cruises as a function of field-observed WS and SST (Tseng et al., 2009):

$$\mathrm{MLD(m)} = 89.3(\pm 65.4) + 5.2(\pm 1.8) \times \mathrm{WS} - 3.2(\pm 2.1) \times \mathrm{SST},$$
$$r^2 = 0.61,\ N = 19,\ p < 0.001 \quad (4)$$

A negative linear relationship was reported between the concentration of (N+N) in the mixed layer and SST below about 26 °C (Tseng et al., 2009):

$$[N+N](\mu M) = -0.11(\pm 0.03) \times SST + 2.95(\pm 0.64),$$
$$r^2 = 0.80,\ N = 7,\ p < 0.001 \quad (5)$$

A similar relationship was found between the concentration of SRP in the mixed layer and SST:

$$SRP(\mu M) = -0.005(\pm 0.001) \times SST + 0.14(\pm 0.03)$$
$$r^2 = 0.6,\ n = 19,\ p < 0.001 \quad (6)$$

Assuming that these relationships are also applicable to conditions from 1997 to 2001, we calculated the MLD and the mixed-layer nutrients and plotted them in Figs. 3a and b. We also calculated the IPP at the SEATS station using SeaWiFS S-chl and PAR for the same period of time (Fig. 3c). The strong seasonal fluctuations of these parameters are well represented. During the 1997–1998 El Niño event, the MLD was estimated to be only 45 m in the 1997–1998 winter and 20 m in the 1998 summer; the (N+N) and SRP in the mixed layer were estimated to be ~0.1 and ~0.02 μM during the 1997–1998 winter and <0.01 and <0.005 μM during summer 1998. These shallower MLD relative to an approximately constant TND of 55 m and lower (N+N) concentrations would be consistent with the suppressed S-chl during the El Niño event (Figs. 3d and 5c).

Based on the above calculated results, anomalies in MLD (MLDA), N+N (N+N A), SRP (SRPA) and MIP (MIPA) were computed according to the method section of "environmental anomalies" (Fig. 7). The MLD anomalies varied between −20 and 10 m between 1997 and 2001 (Fig. 7a). The MLD was below the climatological mean by as much as 20 m during the 1997–1998 El Niño winter. It suggested that vertical convective activity of warming surface waters was much reduced in the weaker winter monsoon (Fig. 5a) under a stronger stratification due to the warming SST (Fig. 5a). The same mechanism probably also accounted for a less pronounced second negative MLDA in the summer associated with a weakened southwest monsoon (Fig. 5a) and warmer than usual SST (Fig. 5b).

Anomalies in N+N and SRP of the surface mixed layer varied between −0.1 and 0.05 and between 0.003 and −0.006 μM, respectively, between 1997 and 2001 (Fig. 7b). The anomaly pattern in N+N and SRP in the surface mixed layer corresponded approximately to those in the MLDA during the winter and summer of the 1997–1998 El Niño. Apparently, nutrient levels in the surface mixed layer decreased during the weaker winter and summer monsoon because of the reduced vertical mixing and enhanced stratification. Nutrients in the upper nutricline were thus less available for supporting photosynthetic activity so that the phytoplankton biomass and production was reduced anomalously. As shown in Fig. 7c, the strongest negative anomalies in IPP (~120 mg-C/m^2/d) both at the SEATS station and in the northern SCS were observed during the winter of the 1997–1998 El Niño. Both IPP anomalous patterns changed in phase closely, corresponding to that in S-chl. (Figs. 5c and 7c). These anomalies were consistent with the reduced vertical advection during the El Niño events as a result of the reduced monsoon strength. According to model exercises (Liu et al., 2002, 2007) monsoon-driven upwelling was critical to the primary productivity in the SCS. As a result, the supply of nutrients to and thus the phytoplankton biomass in the euphotic zone were reduced under a weak winter monsoon. It has been successfully simulated (Wang, 2007) that the reduced wind speed and reversal of heat flux from heat loss to heat gain by the surface ocean during the El Niño resulted in strong depletion of primary productivity at the SEATS station due to reduced vertical mixing. It is noteworthy that upwelling-induced phytoplankton bloom off the northwest Luzon declined dramatically during the 1997–1998 El Niño winter (Fig. 6). The S-chl and IPP estimated for the upwelling region (118–120°E, 18–20°N) dropped by more than half of the normal year winter value. This suggests that upwelling of the cold, nutrient-rich subsurface waters was probably significantly weakened. A more quantitative assessment of how each of the processes, namely, basin-wide upwelling, localized upwelling and upper water column mixing, contributes to the dramatic decrease in nutrient supply during the El Niño event warrants future investigation. How the processes that caused the reduction in biomass and primary productivity in the northern SCS may resemble or differ from those occurring in the central and eastern Pacific regions are discussed next (Chavez et al., 1999; Strutton and Chavez, 2000; Turk et al., 2001; Chavez et al., 2002a, b; Kutsuwada and McPhaden, 2002; Wang et al., 2005b, 2006).

4.3. *Differences between the northern SCS and the equatorial Pacific*

We made comparisons between the SEATS site in the SCS and the WPWP region in terms of seasonality and the biogeochemical conditions in the 1997–1998 El Niño winter (Table 1). The results show large differences in the seasonality, i.e., strong seasonality at the SEATS and weak in the warm pool. The warm pool is basically characterized by weak winds, high SST and low S-chl associated with weak advection and a shallow mixed layer as described in previous reports (McPhaden and Hayes, 1991; Siegel et al., 1995; Ohlmann et al., 1998).

Despite the differences, the inter-annual variation of SST at the SEATS station followed closely the WP index (Figs. 4b and c, Table 2). The significant correlation between SSTA values of SEATS and WPWP indicates the SCS, as a marginal sea of the western tropical Pacific, was certainly impacted by the El Niño event, which was intimately associated with the extent of the WPWP variability. Yet the S-chl anomaly at the SEATS station during the 1997–1998 El Niño event was opposite to that recorded in the WPWP region (Fig. 5c).

The reduction in S-chl at the SEATS station in the 1997–1998 winter was as much as 50% of the average winter level (Table 1). The degree of S-chl reduction was similar to that (−43%) observed in the Niño3 region (Table 1), while the WPWP region underwent a 10% increase in S-chl (Table 1). The SST in the WPWP region

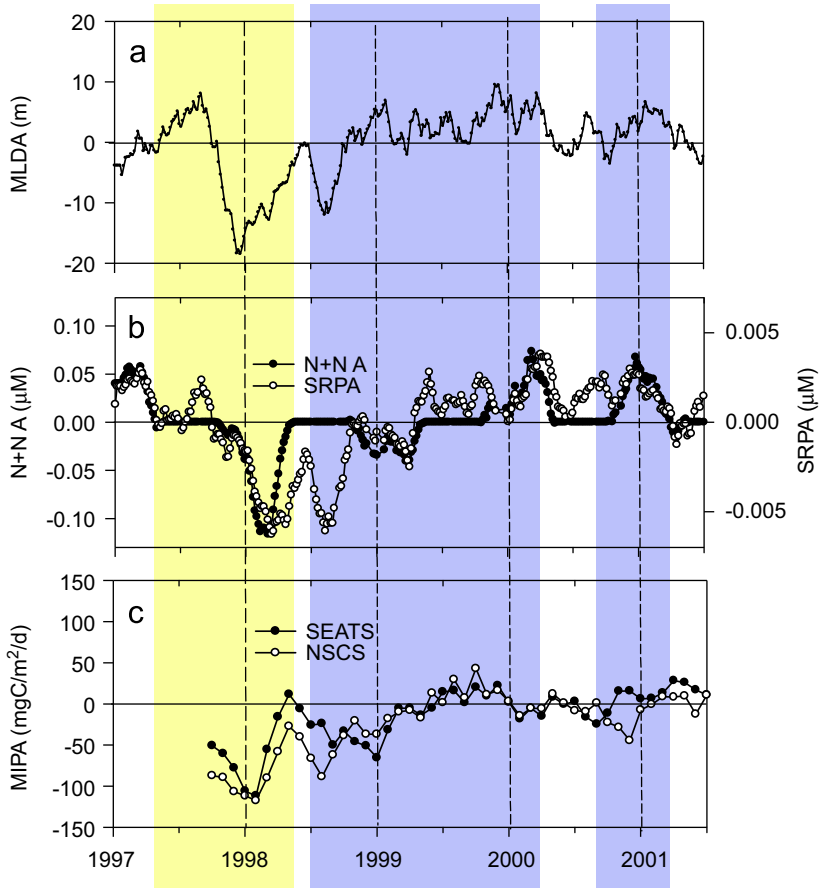

Fig. 7. Anomalies in (a) MLD (MLDA, —), (b) N+N (N+N A, -●-) and SRP (SRPA, -○-), (c) MIP (MIPA at SEATS, -●- and in NSCS, -○-) between January 1997 and December 2001. The ENSO events are marked as in Fig. 2.

was slightly above average by 0.2 °C and the mean WS was also slightly higher by 0.1 m/s. The slightly stronger wind might have contributed to the slightly enhanced S-chl in the WPWP region, but the significantly elevated 20 °C isotherm from an average of 175 to 125 m (Turk et al., 2001; Wang et al., 2006) could be more important. Since uplift of the 20 °C isotherm suggests shoaling of the nutricline, such a change could have strengthened the vertical nutrient supply so as to enhance the surface biological production. Such a process was apparently controlled by large-scale ocean dynamics across the equatorial Pacific. Although the SSTA in the northern SCS appeared to follow the WP index, there is no evidence indicating that the ocean interior dynamics occurring in the WPWP region should have influenced the SCS.

The severe S-chl depletion in the northern SCS during the 1997–1998 El Niño event resembled that in the eastern equatorial Pacific, but the strong and abrupt bounce-back of S-chl that occurred in the Niño3 region (Figs. 3 and 5c) in the summer of 1998 did not occur in the SCS. Such a difference reflected the distinction in upper ocean dynamics between the two systems. The ups and downs of biological production in the eastern equatorial Pacific were controlled mainly by the on-and-offs or reversals of the upwelling-favorable trade wind (Chavez et al., 1999). Although the wind-driven upwelling is also important in the SCS, the upwelling is more localized and considerably weaker (Liu et al., 2002). As discussed earlier, the diminished S-chl was attributed to weakened wind mixing and intensified stratification. It is conceivable that the water column properties in a confined basin, such as the SCS, could not respond to changes in atmospheric conditions quickly. This may explain the lack of S-chl recovery in the northern SCS, even though the wind was strengthened in mid 1998 (Fig. 5a). However, further investigation is warranted.

5. Conclusions

During the 1997–1998 El Niño event, SST was elevated by up to about 2 °C relative to the climatological mean in the northern SCS. Concomitantly, WS and S-chl were decreased by about a quarter and a half, respectively, relative to their climatological means. Additionally, the modeled IPP estimated for the northern SCS area (112–119°E, 15–21°N) was reduced by about 40% of the normal winter. It has been demonstrated that the anomalies had been caused by the weakened wind mixing due to the reduced monsoon strength. The resulting

weakening of vertical mixing probably then led to not just warming of the surface water but also a reduction in the supply of nutrients and thus decline of phytoplankton biomass and production. Based on relationships observed between water column parameters and environmental conditions, we estimated the mixed-layer depth to be only 45 m during the 1997–1998 winter, 30% less than the winter average, and estimated the mixed-layer nutrients to be less than half of the winter averages. Therefore, the reduction of the mixed-layer depth made it ineffective for the nutrients in the upper nutricline to be entrained to the surface layer for fueling phytoplankton growth during the El Niño winter. Thus, the very strong 1997–1998 El Niño event had altered the hydrological and biological conditions in the northern SCS significantly.

The onset of the warming in the northern SCS lagged behind those in the eastern Pacific by about 5 months, and it lingered on for an additional 11 months in a pattern resembling the warm pool index, which is significantly correlated with the SST anomaly of the northern SCS from 1986 to 2003. This suggests that the western Pacific warm pool oscillation plays a critical role in affecting the environmental conditions in the SCS during an El Niño event. However, the ocean interior dynamics that caused uplifting of the 20 °C isotherm in the warm pool region during the 1997–1998 El Niño event and, consequently, enhancement of biological growth, did not show a discernible effect on the northern SCS. The reduction of sea surface chlorophyll in the northern SCS during the 1997–1998 El Niño event was as severe as that in the eastern equatorial Pacific, but the dramatic recovery of sea surface chlorophyll that occurred in the eastern equatorial Pacific in the summer of 1998 did not happen in the SCS. These contrasts reflect the fundamental difference between the biogeochemical systems of the SCS and the eastern equatorial Pacific.

Acknowledgements

We thank the officers and the crew of the R/V Ocean Researcher I and R/V Ocean Researcher III for their assistance in sampling during the SEATS cruises. G.T.F Wong, I.I. Lin and Y. Yang provided critical comments and discussion. T.-D. Sue, P.-W. Chiang, Y.J. Wang and L.-F. Huang assisted in nutrient, chlorophyll and primary productivity measurements. This work was supported by the National Science Council (Taiwan, Republic of China) through grant numbers NSC-93(-94, -95, -96)-2611-M-002-017(-019, -023, -007) and 95-2611-M-019-020,021-MY3 (Center for Marine Biotechnology and Bioscience at National Taiwan Ocean University).

Appendix. Abbreviations, acronyms and definitions used throughout the paper

AT(A)	Surface air temperature (Anomaly)
CTD	Conductivity–temperature–depth
ECS	East China Sea
ENSO	El Niño-Southern Oscillation
EOF	Empirical orthogonal function
EZD	Euphotic zone (PAR >1% of the surface value) depth
GES-DAAC	Goddard Earth Sciences-Distributed Active Archive Center
I-chl	Euphotic zone depth-integrated inventory of chlorophyll-*a*
IPP	Euphotic zone depth-integrated inventory of primary production
MIP(A)	Monthly averaged integrated primary production (Anomaly)
MLD(A)	Mixed-layer (σ_θ gradient $\leq 0.1\ m^{-1}$) depth (Anomaly)
NCEP	National Center for Environmental Prediction
N+N (A)	Nitrate+nitrite (Anomaly)
NASA	National Aeronautics and Space Administration
NOAA	National Oceanic and Atmospheric Administration
PAR	Photosynthetically available radiation
S-chl(A)	Sea surface chlorophyll-*a* (Anomaly)
SCS(WC)	South China Sea (Warm Water)
SEATS	SouthEast Asian Time-series Study
SeaWiFS	Sea-viewing Wide Field-of-view Sensor
SRP(A)	Soluble reactive phosphate (anomaly)
SST(A)	Sea surface temperature (Anomaly)
$SSTA_{N3.4}$	Monthly SST anomaly in Niño 3.4 region
TND	Depth at the top of the nutricline
WP index	Warm pool index as 1st EOF of SST in the WPWP region
WPS	West Philippine Sea
WPWP	Western Pacific warm pool
Winter (DJF)	December–January–February
WS(A)	Wind speed (Anomaly)
ZMCW	Zhe-Min Coastal Water

References

Centurioni, L.R., Niiler, P.P., Lee, D.K., 2004. Observations of inflow of Philippine Sea surface water into the South China Sea through the Luzon Strait. Journal of Physical Oceanography 34 (1), 113–121.

Chao, S.Y., Shaw, P.T., Wu, S.Y., 1996. El Niño modulation of the South China Sea circulation. Progress in Oceanography 38, 51–93.

Chavez, F.P., Strutton, P.G., Friederich, C.E., Feely, R.A., Feldman, G.C., Foley, D.C., McPhaden, M.J., 1999. Biological and chemical response of the equatorial Pacific Ocean to the 1997–98 El Niño. Science 286, 2126–2131.

Chavez, F.P., Collins, C.A., Huyer, A., Mackas, D., 2002a. El Niño along the west coast of North America. Progress in Oceanography 54, 1–5.

Chavez, F.P., Pennington, J.T., Castro, C.G., Ryan, J.P., Michisaki, R.P., Schlining, B., Walz, P., Buck, K.R., McFadyen, A., Collins, C.A., 2002b. Biological and chemical consequences of the 1997–1998 El Niño in central California waters. Progress in Oceanography 54, 205–232.

Feely, R.A., Takahashi, T., Wanninkhof, R., McPhaden, M.J., Cosca, C.E., Sutherland, S.C., Carr, M.E., 2006. Decadal variability of the air-sea CO2 fluxes in the equatorial Pacific Ocean. Journal of Geophysical Research—Oceans 111101029/2005JC003129.

Glantz, M.H., 1996. In: Currents of Change: El Niño's impact on Climate and Society. Cambridge University Press, Cambridge, UK 194pp.

Gong, G.-C., Liu, K.-K., Liu, C.-T., Pai, S.-C., 1992. Chemical hydrography of the South China Sea and a comparison with the West Philippine Sea. Terrestrial Atmospheric Oceanic Sciences 3, 587–602.

Gong, G.-C., Wen, Y.-H., Wang, B.-W., Liu, G.-J., 2003. Seasonal variation of chlorophyll a concentration, primary production and environmental conditions in the subtropical East China. Deep-Sea Research II 50, 1219–1236.

Hoerling, M.P., Whitaker, J.S., Kumar, A., Wang, W., 2001. The midlatitude warming during 1998–2000. Geophysical Research Letters 28, 755–758.

Joseph, J., Miller, F., 1989. El Niño and the fishery for tunas in the eastern Pacific. Bulletin of the Japanese Society of Fisheries Oceanography 53, 77–80.

Kuo, N.J., Ho, C.R., 2004. ENSO effect on the sea surface wind and sea surface temperature in the Taiwan Strait. Geophysical Research Letters 31, L13309, doi:10.1029/2004GL020303 2004.

Kutsuwada, K., McPhaden, M., 2002. Intraseasonal variations in the upper equatorial Pacific Ocean prior to and during the 1997–98 El Niño. Journal of Physical Oceanography 32, 1133–1149.

Liu, C.T., Liu, R.J., 1988. The deep current in the Bashi Channel. Acta Oceanographica Taiwanica 20, 107–116.

Liu, K.-K., Chao, S.-Y., Shaw, P.-T., Gong, G.-C., Chen, C.-C., Tang, T.-Y., 2002. Monsoon-forced chlorophyll distribution and primary production in the South China Sea: observations and a numerical study. Deep-Sea Research I 49, 1387–1412.

Liu, K.-K., Chen, Y.-J., Tseng, C.-M., Lin, I.-I., Liu, H.-B., Snidvongs, A., 2007. The significance of phytoplankton photo-adaptation and benthic-pelagic coupling to primary production in the South China Sea: observations and numerical investigations. Deep-Sea Research II 54 (14–15), 1546–1574.

Liu, K.-K., Tseng, C.-M., Wu, C.-R., Lin, I.-I., 2009. South China Sea. In: Liu, K.K., Atkinson, L., Quiñones, R., Talaue-McManus, L. (Eds.), Carbon and Nutrient Fluxes in Continental Margins: A Global Synthesis. Springer, Berlin In press.

McClain, C.R., Murtugudde, R., Signorini, S., 1999. A simulation of biological processes in the equatorial Pacific Warm Pool at 165 degrees E. Journal of Geophysical Research—Oceans 104 (C8), 18305–18322.

McPhaden, M.J., Hayes, S.P., 1991. On the variability of winds, sea-surface temperature, and surface-layer heat-content in the western Equatorial Pacific. Journal of Geophysical Research—Oceans 96 (S1), 3331–3342.

McPhaden, M.J., Picaut, J., 1990. El Niño-Southern Oscillation displacements of the western equatorial Pacific warm pool. Science 250, 1385–1388.

Murtugudde, R.G., Signorini, S.R., Christian, J.R., Busalacchi, A.J., McClain, C.R., Picaut, J., 1999. Ocean color variability of the tropical Indo-Pacific basin observed by SeaWiFS during 1997–1998. Journal of Geophysical Research 104 (C8), 18351–18366.

Newell, W.H., Weare, B.C., 1976. Ocean temperatures and large scale atmospheric variations. Nature 162, 40–41.

Ohlmann, J.C., Siegel, D.A., Washburn, L., 1998. Radiant heating of the western equatorial Pacific during TOGA-COARE. Journal of Geophysical Research—Oceans 103, 5379–5395.

Picaut, J., Delcroix, T., 1995. Equatorial wave sequence associated with warm pool displacements furignthe 1986–1989 El Niño-La Niña. Journal of Geophysical Research 100, 393–408.

Picaut, J., Loualalen, M., Menkes, T., Delcroix, T., McPhaden, M.J., 1996. Mechanism of the zonal displacements of the Pacific warm pool: implications for ENSO. Science 274, 1486–1489.

Pai, S.-C., Yang, C.-C., Riley, J.P., 1990. Formation kinetics of the pink azo dye in the determination of nitrite in natural waters. Analytica Chimica Acta 229, 115–120.

Qu, T.D., Girton, J.B., Whitehead, J.A., 2006. Deepwater overflow through Luzon Strait. Journal of Geophysical Research—Oceans 111, C01002.

Shang, S., Zhang, C., Hong, H., Liu, Q., Wong, G.T.F., Hu, C., Huang, B., 2005. Hydrographic and biological changes in the Taiwan Strait during the 1997–98 El Niño winter. Geophysical Research Letters 32, L11601, doi:10.1029/2005GL022578.

Shaw, P.T., 1991. The seasonal-variation of the intrusion of the Philippine Sea-water into the South China Sea. Journal of Geophysical Research 96, 821–827.

Shaw, P.T., Chao, S.Y., 1994. Surface circulation in the South China Sea. Deep-Sea Research I 41, 1663–1683.

Shaw, P.T., Chao, S., Liu, Y.K.K., Pai, S.C., Liu, C.T., 1996. Winter upwelling off Luzon in the northeastern South China Sea. Journal of Geophysical Research 101, 16435–16448.

Siegel, D.A., Ohlmann, J.C., Washburn, L., Bidigare, R.R., Nosse, C.T., Fields, E., Zhou, Y.M., 1995. Solar-radiation, phytoplankton pigments and the radiant heating of the equatorial Pacific warm pool. Journal of Geophysical Research-Oceans 100, 4885–4891.

Strickland, J.D.H., Parsons, T.R., 1984. A Practical Handbook of Seawater Analysis, third ed Bulletin of Fisheries Research Board, Canada, Ottawa 311pp.

Strutton, P.G., Chavez, F.P., 2000. Primary productivity in the equatorial Pacific during the 1997–1998 El Niño. Journal of Geophysical Research 105, 26089–26101.

Touree, Y.M., White, W.B., 1997. Evlution of the ENSO signal over the Indo-Pacfic domain. Journal of Physical Oceanography 27, 683–696.

Trenberth, K.E., 1997. The definition of El Niño. Bulletin of the American Meteorological Society 78, 2771–2777.

Tseng, C.M., Wong, G.T.F., Lin, I.I., Wu, C.-L., Liu, K.K., 2005. A unique pattern in phytoplankton biomass in low-latitude waters in the South China Sea. Geophysical Research Letters 32, L08608, doi:10.1029/2004GL022111.

Tseng, C.-M., Wong, G.T.F., Chou, W.-C., Lee, B.-S., Sheu, D.D., Liu, K.-K., 2007. Temporal variations in the carbonate system in the upper layer at the SEATS station. Deep-Sea Research II 54 (14–15), 1448–1468.

Tseng, C.-M., Gong, G.-C., Wang, L.-W., Liu, K.-K., Yang, Y., 2009. Anomalous biogeochemical conditions in the northern South China Sea during the El-Niño events between 1997 and 2003. Geophysical Research Letters 36, L14611, doi:10.1029/2009GL038252.

Turk, D., McPhaden, M.J., Busalacchi, A.J., Lewis, M.R., 2001. Remotely sensed biological production in the equatorial Pacific. Science 293, 471–474.

Wang, D.X., Xie, Q., Du, Y., Wang, W.Q., Chen, J., 2002. The 1997–1998 warm event in the South China Sea. Chinese Science Bulletin 47, 1221–1227.

Wang, J., 1986. Observation of abyssal flows in the northern South China Sea. Acta Oceanographica Taiwanica 16, 36–45.

Wang, P.X., Clemens, S., Beaufort, L., Braconnot, P., Ganssen, G., Jian, Z., Kershaw, P., Sarnthein, M., 2005a. Evolution and variability of the Asian monsoon system: state of the art and outstanding issues. Quaternary Science Reviews 24 (5–6), 595–629.

Wang, X.J., Christian, J., Murtugudde, R., Busalacchi, A., 2005b. Ecosystem dynamics and export production in the central and eastern equatorial Pacific: a modeling study of impact of ENSO. Geophysical Research Letters 32101029/2004GL021538.

Wang, X.J., Christian, J.R., Murtugudde, R., Busalacchi, A.J., 2006. Spatial and temporal variability in new production in the equatorial Pacific during 1980–2003: physical and biogeochemical controls. Deep-Sea Research II 53, 677–697.

Wang, L.-W., 2007. Inter-annual variability of marine biogeochemistry at the SEATS site: application of a one-dimensional coupled physical-biogeochemical model. Ph.D. Dissertation, Institute of Marine Geology Chemistry, National Sun Yet-sen University, pp. 110.

Wong, G.T.F., Tseng, C.-M., Wen, L.-S., Chung, S.W., 2007. Nutrient dynamics and N-anomaly at the SEATS station. Deep-Sea Research II 54, 1528–1545.

Wong, G.T.F., Ku, T.-L., Mulholland, M., Tseng, C.-M., Wang, D.-P., 2007. The South East Asian time-series study (SEATS) and the biogeochemistry of the South China Sea—an overview. Deep-Sea Research II 54 (14–15), 1434–1437.

Yan, X.H., Ho, C.R., Zheng, Q., Kiemas, V., 1992. Temperature and size variability of the western pacific warm pool. Science 258, 1643–1645.

You, Y.Z., Chern, C.S., Yang, Y., Liu, C.T., Liu, K.K., Pai, S.C., 2005. The South China Sea, a cul-de-sac of North Pacific intermediate water. Journal of Oceanography 61 (3), 509–527.

Zhao, H., Tang, D.L., 2007. Effect of 1998 El Niño on the distribution of phytoplankton in the South China Sea. Journal of Geophysical Research 112, C02017, doi:10.1029/2006JC003536.